UiO **: University of Oslo**

Lisa Smith

Experiments of Breaking Waves in Pipes and Flumes

Thesis submitted for the degree of Philosophiae Doctor

Department of Mathematics
Faculty of Mathematics and Natural Sciences

2018

Preface

This thesis is submitted in the partial fulfillment of the requirements for the degree of *philosopiae doctor* (Ph.D.), at the University of Oslo. The research presented in this thesis is conducted under the supervision of Professor Atle Jensen, Dr. Jostein Kolaas and Associate Professor Johan Kristian Sveen. The work is carried out at the Department of Mathematics, and concerns experimental study of breaking waves. The experiments are carried out in the hydrodynamic laboratory at UiO.

The thesis is a collection of four papers and one report. The introduction describes the motivation of the present study, and relates the papers together. The main body of the thesis consists of four journal papers and a report, in chronological order. I am first author on all papers, and was involved in all processes of the research. The research was done as part of the research project *DOMT - developments in optical measurement techniques* funded by The Research Council of Norway (project number 231491).

▮Lisa Smith
Oslo, January 2018

Acknowledgements

Contents

Chapter 1

Introduction

Wave breaking is a physical process that appears frequently in the ocean and when waves travel on shore. It is easily sighted by the white caps tumbling down the front face of the waves, or by the white foam generated as the waves swash upward the beach. It is known that wave breaking is a crucial mechanism for air-sea interaction (Melville, 1996) and is important for transfer of momentum, heat exchange, vapor generation, and dissolution of CO_2 in the sea. These effects have large impact on the weather and on climate changes, but can also disturb ocean wildlife that is dependent on the acidity of the seawater, e.g. blue mussels (Bibby et al. (2008)) and clownfish (Dixson et al. (2010)). Wave breaking can cause damages on structures located in onshore and offshore regions, due to the large forces generated when the waves break. Breaking wave on beaches is also one of the primary reasons for sediment transport on shore (Elfrink and Baldock, 2002). One might think that breaking waves only occur in the ocean and near coastal regions, but wave breaking also appears in man-made installations such as pipelines, and other transportation system of liquids and gases. In most industry today, pipelines and transport systems of fluids are frequently installed. Breaking waves and other violent flow regimes, such as slug flow, can exert large forces on pipelines that will require expensive and robust installation equipment. Knowledge on wave and fluid motion in pipes is therefore highly valued. Especially in Norway, where valuable gas is transported from the North sea to the continent by a large pipeline network (Rømo et al., 2009). It is important to acknowledge some of the discrepancy between wave breaking evolving in natural setting and wave breaking evolving in controlled environments. In the ocean, the wave length and amplitude of natural waves may be much larger than for waves generated in a controlled environments e.g pipes and wave flumes. Scale dependent physical properties such surface tension, viscous contributions, and capillary effects are therefore important to address in small scale examination. In addition, the roughness and inclination of and pipes and flumes are often constant in controlled environments whereas the sea bed roughness, and morphology may vary greatly in the ocean.

In this thesis breaking waves are experimentally investigated in both pipes and wave flumes. In the wave flumes the wave breaking is induced by decreasing the water depth, achieved by inserting an inclined beach at the end of the wave flume. In the pipe experiments, imposing a difference between the air and water flow rates in the pipe generates both breaking and non-breaking waves.
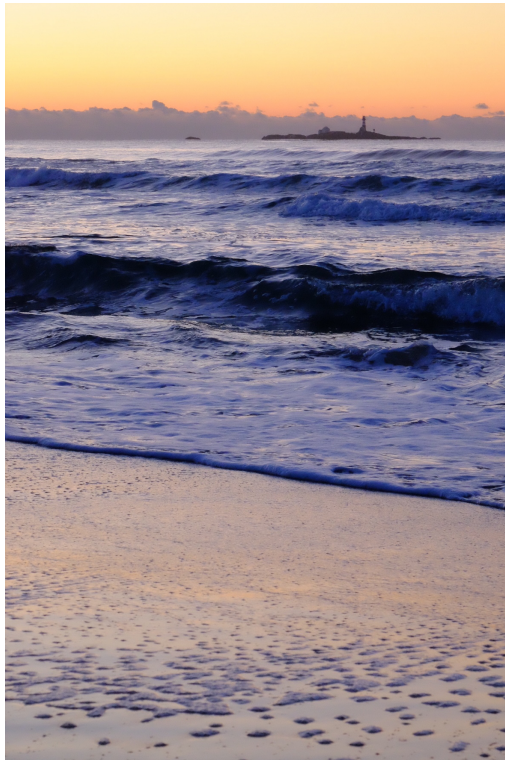
Figure 1.1: Image of breaking waves captured by Ketil Eide at Hellestø, Rogaland

1.1 Breaking waves

Natural wave breaking occurs in the open ocean, and in regions near the coastline. In wave research, we usually divide the breaking waves into two regimes, deep water breaking waves, where the waves are not affected by the sea bed (Banner and Peregrine, 1993), and shallow water breaking waves where the waves break due to change in water depth (Peregrine, 1983). In deep water, we assume the water depth H to be much larger than the wavelength λ. A breaking criterion for deep water waves was established by Stokes in late 19th century. A wave will necessarily break if the wave crest gets steeper than 120°. Although, this is usually applicable, new research has shown that there are several instabilities that can provoke wave breaking in deep water (Benjamin and Feir (1967), Tanaka (1986)).

As waves travel toward the shore, the water depth H decreases, which reduces the wave speed, and increases the wave amplitude. The waves usually become asymmetrical, which may result in a vertical wave front, or that portions of the wave crest overturn. There are four main breaker types that are defined for breaking waves on beaches (Peregrine, 1983): *Spilling*, *Plunging*, *Collapsing* and
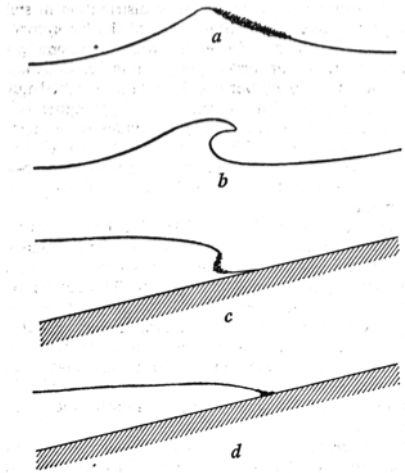
Figure 1.2: Figure of different breaker types. a) Spilling b) Plunging c) Collapsing and d) Surging breakers (Cokelet, 1977)

Surging breakers (Figure 1.2). *Spilling* breakers are characterized as a steep wave, where part of the front face has a turbulent plume with air entrainment. *Plunging* breakers are waves where part of the wave crest is deformed into an overturning jet that eventually reattaches the surface or impinges on a sloped beach. The process can be laminar upon the point of impingement or reattachment. Somewhere in between *spilling* and *plunging* breakers are *collapsing* breakers defined, where the lower part of the wave overturns and creates a turbulent area close to the beach region. The last breaker type is *surging* breakers where most of the surface remains smooth, but a small part of the wave close to the beach is turbulent. The wave has a gentle slope compared to the other breaker types. The first two breaker types are also applicable to deep water breaking.

Breaking waves can also appear in small scale, e.g. micro breaking, where no air is entrained in the waves. If we follow the wave as a frame of reference, the breaking occurs when a stagnation point is present on the surface, or when particle velocities exceed the wave speed. The micro breaking waves are often generated by wind (Banner and Phillips (1974).

Solitary waves are often used to study wave breaking, both numerically and experimentally (Synolakis, 1987). Solitary waves consist of an infinite long single crested wave and can travel on uniform depth without changing shape. The shallow water steepening is therefore balanced by the dispersive effect. Solitary waves can be described by a single parameter, the normalized amplitude $\alpha = A/H$. It is easy to reproduce and is therefore often used as a reference wave in experimental studies. Commonly, experiments are conducted to validate results from a numerical model. A breaking criterion for solitary waves on a

sloping beach was reported by Synolakis (1987)

$$\frac{A}{H} \geq 0.818(\tan\theta)^{10/9}, \qquad (1.1)$$

where θ is the inclination of the beach.

At the department of mathematics at UiO, investigation of runup of nonlinear waves have been studied for decades (Gjevik and Pedersen (1981), Jensen et al. (2003) and Pedersen et al. (2013)). To investigate the runup of solitary waves, a vareity of different numerical models are utilized, Boussinesq (Pedersen and Gjevik, 1983), Navier-Stokes solver (FLUENT)(Wood et al., 2003) and Boundary Integral Model (Pedersen et al., 2013). Discrepancies between the models and experiments are reported, especially for measurements in the last stages of runup, where capillary and viscous effects are prominent (Pedersen et al., 2013). Optical measurements techniques e.g. PIV (Sveen and Cowen, 2004) have been used to investigate velocities in breaking waves Jensen et al. (2005), Grue et al. (2014) and Smith et al. (2017).

Researchers worldwide have used a lot of effort and resources to investigate wave breaking in the latest centuries (Russell, 1845). Both theory and experiments are conducted to gain insight in some of the unanswered questions regarding wave breaking. In addition, field studies have been conducted to connect theory and experiments to real ocean wave breaking, e.g. Sutherland and Melville (2013). Laboratory experiments have been conducted to validate and identify limitations of theoretical and computational models. Optical measurement techniques such as PIV (Chang and Liu (1998), Kimmoun and Branger (2007). Kikkerta et al. (2011), and Belden and Techet (2011)), and bubble image velocimetry (BIV) (Rivillas-Ospina et al., 2012) are used to investigate velocity fields in breaking waves. Chang and Liu (1998) investigated velocities within the plunging jet and found that the velocity in the tip was 1.7 times greater than the phase speed of the wave. Kimmoun and Branger (2007) investigated stages after the plunger had impinged the beach (surf zone), and applied 14 different field of views. Fluctuating velocities was measured using a phase average measurement for 51 wave repetitions. Small scale spilling breaker experiments were conducted by Lucarelli et al. (2017), where a hexapod wave tank system was used to generate waves, which enable steady and repeatable wave condition. 512 repetitions were performed, and statiscal PIV analysis of the turbulent region below the air entrained front was obtained. Kikkerta et al. (2011) measured velocity fields in a bore driven swash, during runup, and investigate how the change in beach roughness effected the velocities. They found that an increase in beach roughness reduced the maximum runup height. In addition they found that roughness effect was limited for uprush, but played a significant role in the start of the backwash. To investigate the air-water interaction, PIV was simultaneously performed in both phases by Belden and Techet (2011). The study revealed that the breaking process introduced vorticity in the air phase. BIV was used to investigate velocities in the swash zone by Rivillas-Ospina et al. (2012). The method is similar to PIV, but does not use tracer particles. Instead, the texture in the images made by air bubbles interfaces, are correlated to find

the velocities. The result was compared to simulation from a RANS (Reynold Average Navier Stokes) model and showed fairy good agreement. Pujara et al. (2015) measured bed shear stresses by a shear plate sensor placed in the swash zone. The experiment revealed that the maximum bed shear stress was during backwash.

To determine the size of the large air cavity enclosed by a plunging breaker, both theoretical and experimental studies are performed. Longuet-Higgins (1982) calculated a cubic parametric curve that fits the shape of the enclosed air cavity formed by plunging breakers, and found that the ratio between the major and minor axis was approximately 2.75. The air bubble characteristics, after wave breaking on a submerged reef, were studied by Blenkinsopp and Chaplin (2007) and Blenkinsopp and Chaplin (2011). They discussed how the submergence of the reef affected the breaker characteristic, e.g. size and distribution of the air bubbles. In the last paper they discussed scale effects in breaking waves with a focus on aeration. Surface tension effects was studied by Stagonas et al. (2011), where two sets of experiments were conducted one with fresh water and one with a 10% isopropyl-alcohol mixture. The weakening of the surface tension seems to increase the energy dissipation with 65% for waves smaller than 11 cm and shorter than 4 m.

Even though, a lot of knowledge is retrieved in the latest decade, still many questions regarding wave breaking remains unanswered. The stages after a strong plunging breaker impinges the beach are still poorly understood. 3D motion, bubble behaviour and turbulence are some of the scopes that need further investigation.

Small scale laboratory experiments can resemble realistic ocean behaviour, but there are some discrepancies between real ocean waves and experimental waves that are important to elaborate. In most experimental work, regular fresh water is used instead of seawater. Seawater is approximately 2.5% denser than fresh water, and the surface tension is one percent higher than fresh water. Also seawater is approximately 7.5 more viscous (Blenkinsopp and Chaplin, 2011). Not all physical mechanisms are scalable e.g. surface tension, which is really important for small scale formation of plunging breaker. In addition, the solitary wave condition is not realistic for real ocean breaking waves.

1.2   Multiphase pipe flow

When fluids are transported in pipes for long distances, a range of different wave regimes can occur. The flow regimes that can be obtained in two phase horizontal pipe flow are shown in Figure 1.3. Figure 1.4 shows the corresponding flow map that classify the different flow regimes based on the superficial flow rates of the system. The flow map classification is to some degree dependent on the experimental settings, and might therefore differ slightly for different flow loops.

Stratified flow is the simplest flow regime, where the fluids are completely separated with a horizontal interface. This flow regime is only present when the
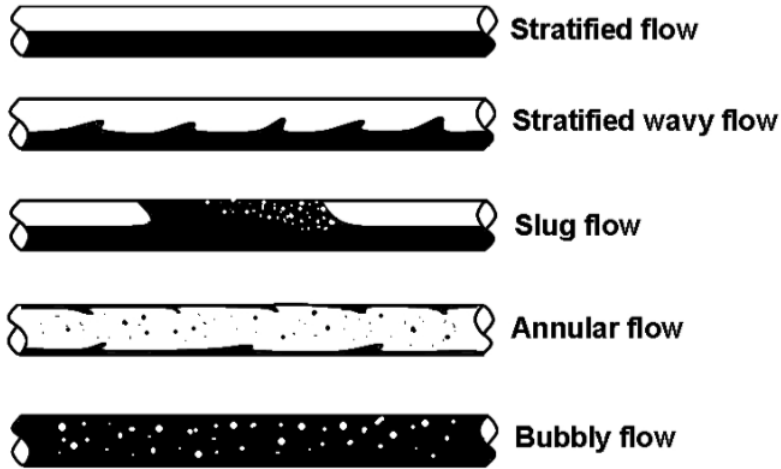
Figure 1.3: Different flow regimes for horizontal pipe flow (Schulkes, 2010).

flow rates are low. If we increase the difference in flow rates of the two phases, an increase in interfacial shear stress occurs, and waves with small amplitude are generated. The stratified wavy flow regime is difficult to model due to the unknown correlation of wall and interfacial shear stresses. The wall shear stresses are usually modeled by Blasius formula, or by Colebrook equation, which concider the pipe roughness. A lot of effort is conducted to find a model for the interfacial shear stresses for wavy flows, (Taitel and Dukler (1976), Andritsos and Hanratty (1987a) and Tzotzi and Andritsos (2013)). The stratified flow regimes (extended definition that includes all regimes where the two phases are completely seperated) can be classified into 4 different regimes (Tzotzi and Andritsos, 2013):

1. No waves are present and a completely horizontal interface is obtained. Lower left region in Figure 1.4

2. Waves with small wavelength, and small amplitudes are observed. Both wavelength and wave amplitude increases with distance of the pipe. Middle lower region in Figure 1.4.

3. Large 2D irregular waves. The waves have a steep wave front and a milder back slope (Roll waves). The transition to this wave regime is related to the Kelvin-Helmoltz instability (Andritsos and Hanratty, 1987b). Middle lower region in Figure 1.4.

Figure 1.4: Flow map for horizontal pipe flow (Schulkes, 2010).

4. Atomization, the liquid is deposited on the pipe walls and air droplets are erupted from the wave crest.
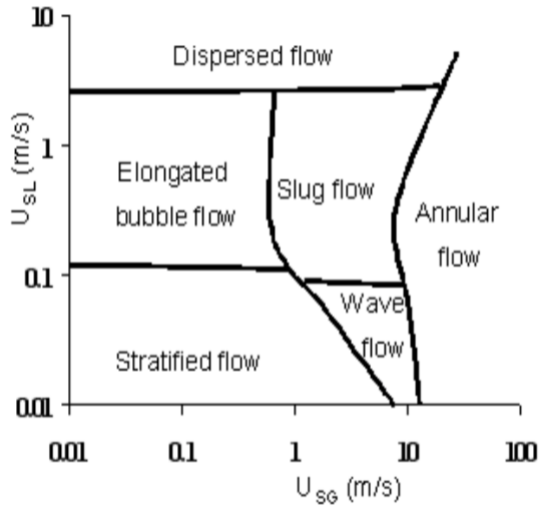
The transition from small amplitude stratified wave flow, to either intermittent slug flow or roll waves are often predicted by the Kelvin- Helmoltz instability (Andritsos and Hanratty, 1987b). The growth rate of the waves is countered by the gravity forces for stable wave regimes. If the growth rate is stronger than the gravity forces, the amplitude may reach a critical level, where the wave crest moves faster than the wave troughs, which may induce wave breaking. At this point the wave has reached it maximum energy (Cokelet, 1977). If the gas velocity is increased at this point, suppression of the liquid will occur, and generate irregular roll waves (Sanchis et al., 2011). However, if the liquid velocity increases, the liquid holdup h_l increases, which decreases the normalized amplitude (A/h_l) of the waves, and the wave may not break. Nevertheless, the increase in liquid hold up might increase the entire water level $h_l + A$, and this may result in a large liquid slug if the water level occupies the entire pipe diameter. This is the start of slugs formation.

Most of the experimental work conducted at the hydrodynamics laboratory at UiO concerns horizontal stratified wavy pipe flow. A range of different measurement techniques e.g. conductance probes (Strand, 1993), PIV (Ayati et al. (2014), Ayati et al. (2015)), hot wire measurements (Ayati et al., 2016) and optical investigation Sanchis et al. (2011) have been utilized to establish physical parameters such wave amplitude, wave spectra, and velocities in both liquid and gas phase Ayati et al. (2015).

Worldwide, a range of different measurement techniques is applied to investi-

gate multiphase flow phenomenon. In addition to the methods mentioned above, a selection of method is X-ray and gamma measurement (Hu et al. (2005) Fischer and Hampel (2010) and Hoffmann and Johnson (2011)), and Doppler Anemomentry measurements (Sheng and Irons, 1991). The latter study used both Doppler Anemometry and electrical wires to investigate bubbly flows. Czapp et al. (2012) developed a stereo PIV method to investigate velocities in slugs. In slug research, mostly statistical quantities such as slug length, slug frequency, and holdup are reported (Nydal et al., 1992). Short slugs collaps as they travel in a horizontal pipe and the relationship between slug length and collapse rate are studied by Cook and Behnia (2000).

Even though, a large amount studies on multiphase flow have been conducted in the latest century, many questions are still unanswered. Especially, questions regarding flow transition are still not adequately understood. The wavy flow interfacial stress models may be further developed to improve estimates on flow properties and flow transition. Moreover, the dynamics in slug flow are still poorly understood.

Chapter 2

Experimental work

There are three main experimental setups in this thesis. The first setup was in the large wave tank facility in the hydrodynamics laboratory at UiO, where acoustic surface elevation measurements and PIV measurements of boundary layers within breaking solitary waves were conducted. The steepest breaking waves were generated in the second experimental setup, but in a much smaller wave flume. The small scale facility was approximately 7 times smaller than the large wave tank facility. The size of the small scale experiments was determined by limitation in the X-ray system strength. X-ray measurements and acoustic surface elevation measurements was performed. Images from the wave flume experiments are shown in 2.1. The final experimental setup is the large flow loop in the hydrodynamics laboratory. X-ray measurement and conductance probe measurements are conducted. In following section, a short description of the different measuring technique will be provided.

2.0.1 Ultrasonic wave probes

Surface elevation measurements are conducted with non-intrusive acoustic wave probes. The probes emit ultrasonic pulses toward a surface that reflects the
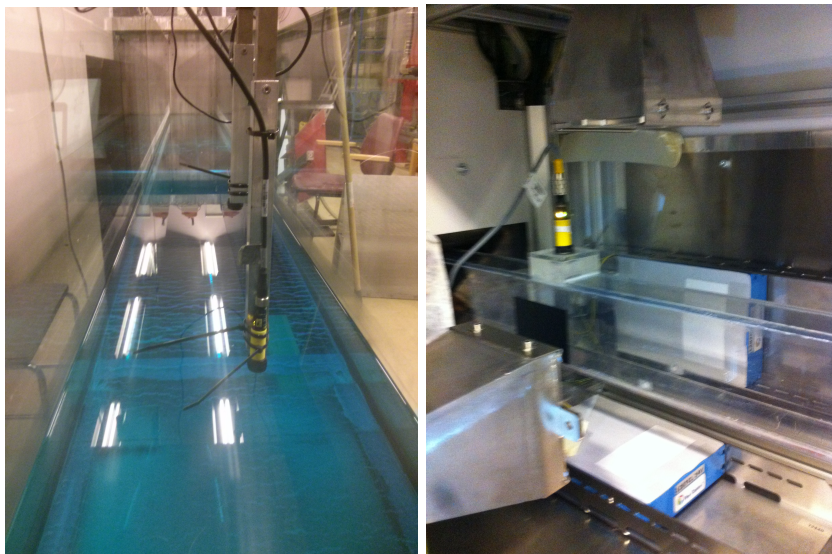

Figure 2.1: Left: Image from the large wave flume. Right: Image from the small wave flume

signal back to the probes. The pulses travel with the speed of sound, and the distance to the surface is calculated based on the time from output to input. The probe needs calibration at different water levels. One of the drawbacks with this measuring device is its inability to measure steep waves. If the ultra sonic signal is reflected by a steep interface, the signal will be reflected in a different direction, and will not be detected by the sensor. This leads to dropouts in the measurements. This is really problematic in breaking wave investigation, since the waves usually have a steep wave front before breaking.

2.1   PIV and PTV

To measure velocity in flows, the non-intrusive optical measurement techniques, Particle Image Velocimetry (PIV) and Particle Tracking Velocimetry (PTV) are performed. The equipment needed for the the two techniques is equivalent. A high speed camera, a 2D light sheet generated by a flashing laser, and tracer particles suspended in the fluid. The particles should be sufficiently small, neutrally buoyant and follow the flow as passive tracers. An image of the PIV setup is provided in Figure 2.2. The right image shows a breaking wave where particles are suspended in the fluid.

The PTV algorithm matches particles in an image to particles detected in a later image, by comparing the particles size, shape and light intensity. The particles are said to be a good match if similarities are found. The algorithm couples particles such that the sum of differencess between all the particle matches is minimized for each of the image pairs. Additional cost functions can be applied, and often previous history of particles is stored and emphasized. The result is a two dimensional unstructured velocity grid.

PIV is a pattern matching technique that use cross correlation to find displacement of particle patterns between two images separated by a time step. The particle images are divided into smaller interrogation regions (subwindows), and a velocity vector is obtained for each subwindow. For the subwindows in the first image, correlation to subwindows within a fixed region in the second image are calculated. This gives us a correlation plane as a function of window shift. The window shift with the highest correlation is the subwindow displacement with best particle pattern match. More details regarding the PIV and PTV techniques can be found in Dalziel (1992) or in Sveen (2004).

2.2   X-ray measurement techniques

X-rays were first reported and detected by Wilhelm Röntgen in the late 19th century. X-rays have the ability to propagate through soft tissue, and can visualize structures inside opaque objects. X-rays have wavelengths that are smaller than optical light and range from $0.01\,\text{nm}$ to $10\,\text{nm}$. X-rays are ionizing radiation and may be harmful for humans and animals. It is therefore important to be cautious when working with X-rays. Even though X-rays can cause harm to humans, the diagnostic benefits from performing an X-ray examination have
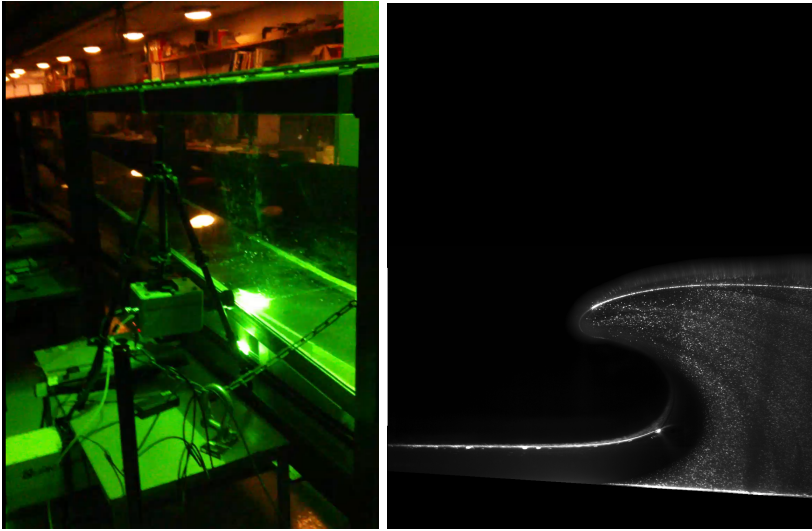
Figure 2.2: Images from the PIV acquisition. Left: Image of the setup. Right: Image from experiment from Mo et al. (2013)

been life saving in many cases. In medicine, X-rays have mostly been used to visualize bones and tissue, and can detect fractures and measure blood supply to different organs. In the latest decades, many new X-ray techniques have been developed, X-ray Computed Tomography (CT) (Hounsfield, 1973) and contrast enhanced techniques (Lewis, 2004), where the shift in phase of the X-rays are measured and related to the tissue properties. A review of in vivo X-ray measurement techniques is available in Fouras et al. (2009).

In the field of fluid mechanics, X-rays and gamma rays are used to investigate flow properties mostly connected to multiphase flow (Heindel, 2011). Void, holdup and flow structures are physical parameters that are investigated (Hoffmann and Johnson (2011) and Hu et al. (2014)). Also, a lot of effort has been made to develop tomographic 3D reconstructions (Hu et al. (2005) and Fischer and Hampel (2010)) to investigate phase distribution in pipe flow. A new development (Drake et al. (2011) and Kertzscher et al. (2004)) is to insert X-ray particles into opaque flows, to measure velocities in regions with limited optical access. The X-ray PTV technique is based on regular PTV as described in section 2.1. The X-ray absorbing particles make an imprint in the X-ray images that can be tracked in an image series. Ideally, the particles should follow the fluid as passive tracers, which implies that they must be neutrally buoyant and small compared to other length scales of the experiment. The stokes number S_{tk} describes the effect of inertia on particles in a fluid flow, and is defined in Paper V. A study from Xu and Bodenschatz (2008) revealed that in turbulent flow, the use of large particles can be adequate if the density difference between the particles and the fluid is small. However the large particles were more prone to cluster. To make
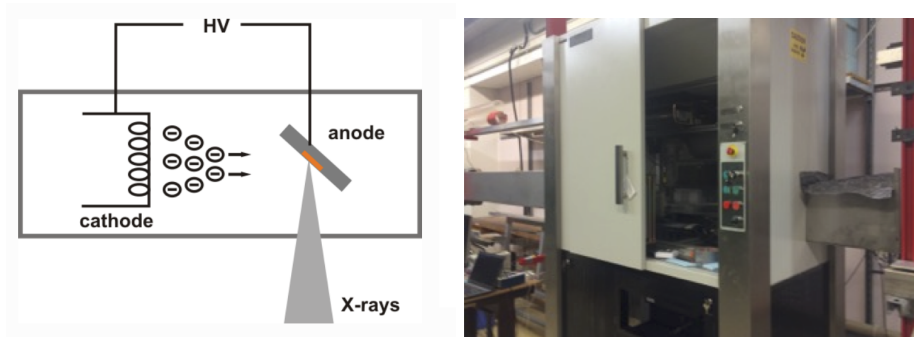
Figure 2.3: Left: Sketch of an X-ray tube. Right: Image of the X-ray cabinet

or find small X-ray absorbing particles with an average density close to water are not an easy task (Drake et al., 2011). Although, difficulties are reported in Paper II and V, a stereographic X-ray technique can measure 3D velocities in a less complicated manner than other available methods e.g. tomographic and stereo PIV Scarano (2012), which both need advanced calibration.

X-rays can be produced and regulated by an X-ray tube. An anode, a cathode, and a tungsten (Wolfram in Norwegian) filament are mounted inside a vacuum tube as shown in the left image in Figure 2.3. A strong current is applied, which heats the cathode, resulting in emitted electrons. The electrons accelerate toward the anode, and hit the tungsten filament. The collision with filament, results mostly in heat, but a small part of the energy is converted to X-ray photons.

The X-ray system utilized in this thesis has a maximum voltage between the anode and the cathode of $80\,kV$. This implies that the maximum X-ray energy of a single X-ray photon cannot exceed $80\,keV$. Three effects are important, when low energetic X-rays interact with matter: coherent scattering, photoelectric effect and Compton scattering (Attix, 2008). High energy effects such as pair production and photon nuclear interaction that occurs in the energy range above 1 MeV, will not be reviewed in this thesis. Coherent scattering occurs when photons have too little energy, to liberate an electron in the outer shells of the atoms. The energy and the wavelength of the photons remains the same, but the photons direction changes. The photoelectric effect, or photon absorption occurs when photons have enough energy to liberate electrons from the atoms shells. The photons are completely absorbed. The amount of photons that are absorbed is dependent on the wavelength of the X-rays, and the density of the material. The absorption increases with increasing density and with decreasing X-ray wavelength. Compton (Incoherent) scattering appears when incoming X-ray photons collide with freely bounded electrons in atoms. The photons are scattered, but also a shift in wavelength (Compton shift) of the photons occurs, and the energy of the photons decreases. The summation of Compton scattering and photon absorption is what we call X-ray attenuation, and is important for

X-ray imaging. The attenuation of monochromatic X-rays that propagate in a uniform media with attenuation coefficient μ can be described by Beers law

$$\frac{I}{I_0} = \exp(-\mu l_x) \tag{2.1}$$

where I_o is the incoming X-ray intensity, and l_x is the length of the X-ray path. The unabsorbed X-ray and and non scattered photons are detected by a CMOS X-ray detector. Calibration is needed for each of the pixels in the detector to find the attenuation coefficient μ^* related to the system. Details regarding the calibration can be found in Paper III.

It should also be mentioned that the X-ray generation, creates heat that must be transported away from the measurement area. If acquisitions occur over a longer period, the temperature inside the X-ray cabinet rises. A fan is installed to transport the heat away from the machine, but at the same time, this creates a vacuum inside the X-ray machine. An image of the X-ray machine is provided in Figure 2.3.

2.2.1 Milk crown experiment

X-ray measurements of a milk crown are conducted to test the sensitivity of the X-ray system, and to do some preliminary tests with the X-ray machine. A droplet of milk is released into a cylindrical container with a diameter of 53 mm filled with 1.4 mm whole milk. The milk droplet size was measured to be 3.5 mm. Images from the top view are shown in Figure 2.4 and images from the side view are show in Figure 2.5. The investigation shows how a single droplet generates a disturbance that develops into a milk crown and then evolves into small erupted droplets. The X-ray system is able to differentiate between air and small droplet. In the first image the droplet falls, and the shape of the droplet appears to be elongated for the top view. This is an artifact, and is due to the relative long exposure time compared to the velocity of the milk droplet. The long exposure time is one of the limitations that was challenging, with the X-ray research conducted in this thesis.

2.3 Conductance probes

The conductance gauge consists of 4 doubled wired conductance probes. Two of the probes are located in the center of the pipe with a distance of 6 cm, and the other two are mounted on each side of the first probe, separated by a 6 cm. The wire's diameter is 0.3 mm, and they are made of platinum. The conductivity of the wire is dependent on the liquid level in the pipe. The probes generate an output voltage signal that needs calibration to relate output and liquid levels. The calibration of the probes is conducted outside of the pipe, in a much smaller pipe, where it was easier to control the liquid level. An image from the calibration is shown in Figure 2.6. The measurement technique is intrusive and small capillary effect may be introduced. More information regarding the conductance probes can be found in Ayati et al. (2014).

Figure 2.4: X-ray measurement from the top view of the droplet before and after the droplets impact on the milk surface. The colorbar represent the normalized X-ray intensity difference from an image with no motion
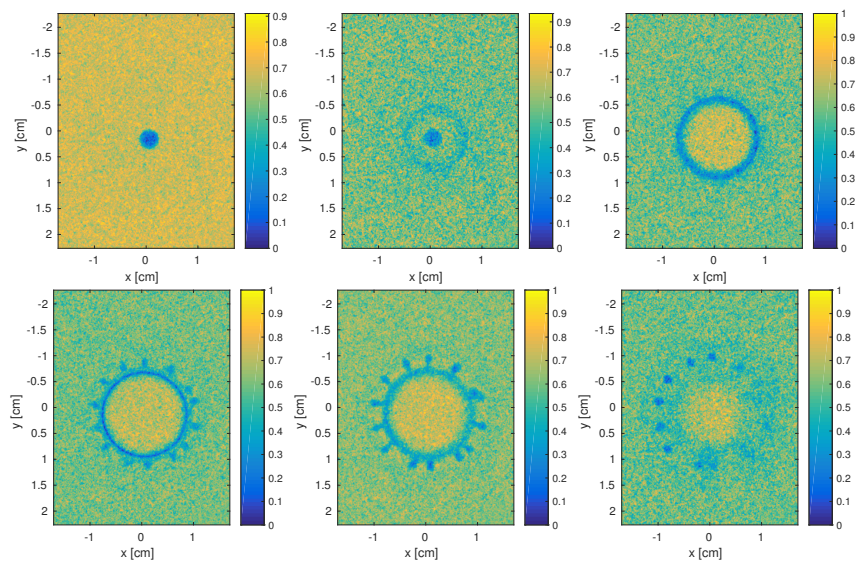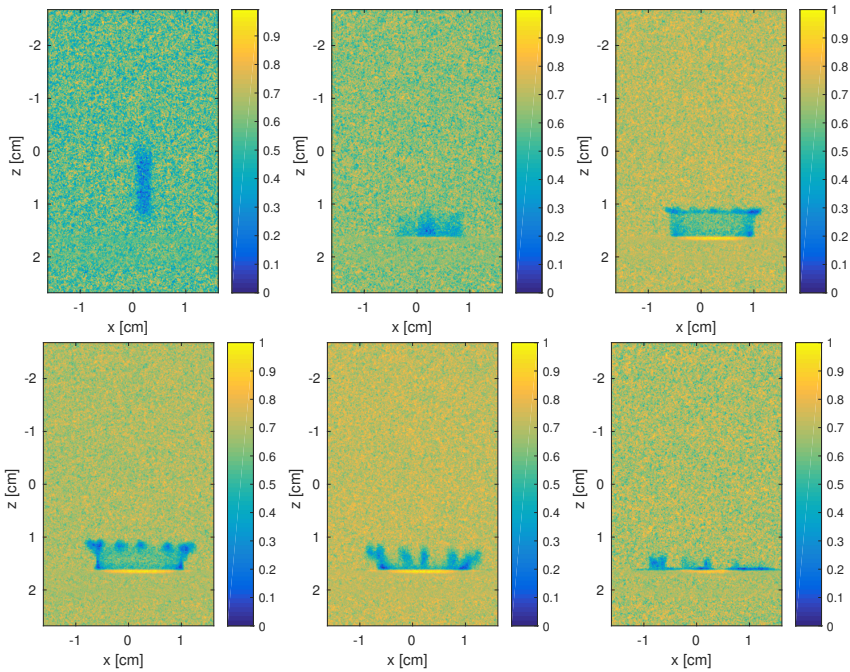
Figure 2.5: X-ray measurement from the side view of the droplet before and after the droplets impact on the milk surface. The colorbar represent the normalized X-ray intensity difference from an image with no motion
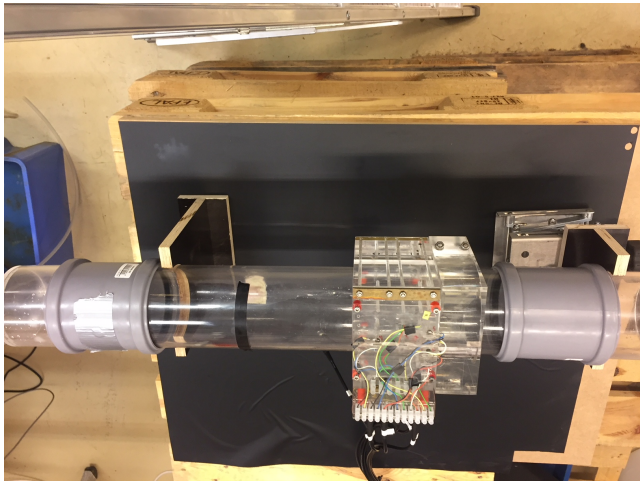

Figure 2.6: Image of the conductance gauge

Chapter 3

Objectives, findings and future perspective

There are three main objectives in this thesis. i) To acquire knowledge about the physics behind wave breaking and dynamics in flows with air-water mixing. ii) Validate an X-ray measurement technique for measuring surface structures and enable 3D tomographic reconstruction. iii) Develop an X-ray PTV system for velocity measurements in high velocity flows with aeration. The relations between the objectives and the papers in the thesis are provided below.

Paper I: Investigation of breaking and non-breaking solitary waves and measurements of swash zone dynamics on a 5° beach

This paper is related to the work conducted by Pedersen et al. (2013), and can be considered as a continuation of their work. The difference between the investigations is the slope of the beach, which was milder for this study. The gentle slope, resulted in plunging breaking waves instead of non breaking waves, and the scope of the study was altered toward wave breaking. Boundary layers, bubble size, and runup were reported, and revealed that irregularity became more prominent further up the beach. This study covers part of the first objective.

Paper II: X-ray PTV Measurements of Solitary Waves

In the hydrodynamics laboratory at UiO, a high speed X-ray system was installed in the spring of 2015. This paper is the first study where the new X-ray system was used. The paper shows some preliminary results of solitary waves measurement. Both surface structures and X-ray PTV were tested and reported (Objectives ii and iii). The X-ray PTV measurements deviated from theoretical result with 23%.

Paper III: X-ray measurements of plunging breaking solitary waves

The experiments conducted in this study are similar to the study of Paper II. A beach was inserted in the end of the wave tank to investigate breaking waves. The X-ray system enabled void measurements in the breaking waves, and 3D reconstruction of the wave. The plunging breaker encapsulated a symmetrical air tube that disintegrated into smaller air bubbles. Two larger air pockets were observed close to the walls of the wave tank. The maximum runup was also reported. The aim of this study is related to the objectives i and ii .

Paper IV: Investigation of surface structures in two phase wavy pipe flow by utilizing X-ray tomography

In this study, waves in pipe were investigated by the X-ray measurement technique. The work is connected to the work performed by Sanchis et al. (2011) and Ayati et al. (2014). Linear wave regimes to non-linear breaking regimes were investigated. The X-ray measurements revealed that the non-linear wave regimes were more asymmetrical. For the breaking wave regime, a one sided breaking wave was observed. Both objectives i an ii was covered in this study.

Paper V: A note on X-ray PTV of slugs in pipes

One of the main issues with the X-ray PTV investigation in Paper II was that the particles sank rapidly towards the bottom of the wave tank. In this study the X-ray particles was inserted into a horizontal pipe with slug flow. Even though, we were able to track particles within the slugs, the analysis of the measurements were limited by the number of repetitions. The work is related to objective iii.

3.1 Future work

There is a myriad of different directions that could be a possible path for future work with the X-ray measurement technique. In the following, some ideas and suggestions of new surveys are outlined. It would be interesting to add a percentage of alcohol to the water in the experiments from Paper III. Then we would be able to decide how the surface tension affects the breaking mechanism. Also if the surface tension was decreased, I presume that it would be easier to control the breaking, and that plunging breakers could be generated with lower amplitudes. This will allow us to investigate different breaking types with different amplitudes, which will make it possible investigate scale effects related to breaking.

For the pipe flow experiments, it would be tempting to do more experiments of slug flow, such that averaged velocities can be obtained. This will make it easier to analyse the data, and to understand the dynamics in slugs.

Bibliography

Andritsos, N., Hanratty, T., 1987a. Influence of interfacial waves in stratified gas-liquid flows. AIChE journal 33 (3), 444–454.

Andritsos, N., Hanratty, T., 1987b. Interfacial instabilities for horizontal gas-liquid flows in pipelines. International journal of multiphase flow 13 (5), 583–603.

Attix, F. H., 2008. Introduction to radiological physics and radiation dosimetry. John Wiley & Sons.

Ayati, A., Kolaas, J., Jensen, A., Johnson, G., 2014. A piv investigation of stratified gas–liquid flow in a horizontal pipe. International Journal of Multiphase Flow 61, 129–143.

Ayati, A., Kolaas, J., Jensen, A., Johnson, G., 2015. Combined simultaneous two-phase piv and interface elevation measurements in stratified gas/liquid pipe flow. International Journal of Multiphase Flow 74, 45–58.

Ayati, A., Kolaas, J., Jensen, A., Johnson, G., 2016. The effect of interfacial waves on the turbulence structure of stratified air/water pipe flow. International Journal of Multiphase Flow 78, 104–116.

Banner, M., Peregrine, D., 1993. Wave breaking in deep water. Annual Review of Fluid Mechanics 25 (1), 373–397.

Banner, M. L., Phillips, O., 1974. On the incipient breaking of small scale waves. Journal of Fluid Mechanics 65 (4), 647–656.

Belden, J., Techet, A. H., 2011. Simultaneous quantitative flow measurement using piv on both sides of the air–water interface for breaking waves. Experiments in Fluids 50 (1), 149–161.

Benjamin, T. B., Feir, J., 1967. The disintegration of wave trains on deep water part 1. theory. Journal of Fluid Mechanics 27 (3), 417–430.

Bibby, R., Widdicombe, S., Parry, H., Spicer, J., Pipe, R., 2008. Effects of ocean acidification on the immune response of the blue mussel mytilus edulis. Aquatic Biology 2 (1), 67–74.

Blenkinsopp, C., Chaplin, J., 2007. Void fraction measurements in breaking waves. In: Proceedings of the Royal Society of London A: Mathematical, Physical and Engineering Sciences. Vol. 463. The Royal Society, pp. 3151–3170.

Blenkinsopp, C., Chaplin, J., 2011. Void fraction measurements and scale effects in breaking waves in freshwater and seawater. Coastal Engineering 58 (5), 417–428.

Chang, K.-A., Liu, P. L.-F., 1998. Velocity, acceleration and vorticity under a breaking wave. Physics of Fluids 10 (1), 327–329.

Cokelet, E., 1977. Breaking waves. Nature 267, 769–774.

Cook, M., Behnia, M., 2000. Slug length prediction in near horizontal gas–liquid intermittent flow. Chemical Engineering Science 55 (11), 2009–2018.

Czapp, M., Muller, C., Fernández, P. A., Sattelmayer, T., 2012. High-speed stereo and 2d piv measurements of two-phase slug flow in a horizontal pipe. In: 16th international symposium on applications of laser techniques to fluid mechanics, Lisbon, Portugal. pp. 9–12.

Dalziel, S. B., 1992. Decay of rotating turbulence: some particle tracking experiments. Applied Scientific Research.

Dixson, D. L., Munday, P. L., Jones, G. P., 2010. Ocean acidification disrupts the innate ability of fish to detect predator olfactory cues. Ecology letters 13 (1), 68–75.

Drake, J. B., Kenney, A. L., Morgan, T. B., Heindel, T. J., 2011. Developing tracer particles for x-ray particle tracking velocimetry. In: ASME-JSME-KSME 2011 Joint Fluids Engineering Conference. American Society of Mechanical Engineers, pp. 2685–2692.

Elfrink, B., Baldock, T., 2002. Hydrodynamics and sediment transport in the swash zone: a review and perspectives. Coastal Engineering 45 (3), 149–167.

Fischer, F., Hampel, U., 2010. Ultra fast electron beam x-ray computed tomography for two-phase flow measurement. Nuclear Engineering and Design 240 (9), 2254–2259.

Fouras, A., Kitchen, M., Dubsky, S., Lewis, R., Hooper, S., Hourigan, K., 2009. The past, present, and future of x-ray technology for in vivo imaging of function and form. Journal of Applied Physics 105 (10), 102009.

Gjevik, B., Pedersen, G., 1981. Run-up of long waves on an inclined plane. Preprint series. Mechanics and Applied Mathematics http://urn. nb. no/URN: NBN: no-23418.

Grue, J., Kolaas, J., Jensen, A., 2014. Velocity fields in breaking-limited waves on finite depth. European Journal of Mechanics-B/Fluids 47, 97–107.

Heindel, T. J., 2011. A review of x-ray flow visualization with applications to multiphase flows. Journal of Fluids Engineering 133 (7), 074001.

Hoffmann, R., Johnson, G. W., 2011. Measuring phase distribution in high pressure three-phase flow using gamma densitometry. Flow Measurement and Instrumentation 22 (5), 351–359.

Hounsfield, G. N., 1973. Computerized transverse axial scanning (tomography): Part 1. description of system. The British journal of radiology 46 (552), 1016–1022.

Hu, B., Langsholt, M., Liu, L., Andersson, P., Lawrence, C., 2014. Flow structure and phase distribution in stratified and slug flows measured by x-ray tomography. International Journal of Multiphase Flow 67, 162–179.

Hu, B., Stewart, C., Hale, C. P., Lawrence, C. J., Hall, A. R., Zwiens, H., Hewitt, G. F., 2005. Development of an x-ray computed tomography (ct) system with sparse sources: application to three-phase pipe flow visualization. Experiments in fluids 39 (4), 667–678.

Jensen, A., Mayer, S., Pedersen, G. K., 2005. Experiments and computation of onshore breaking solitary waves. Measurement Science and Technology 16 (10), 1913.

Jensen, A., Pedersen, G. K., Wood, D. J., 2003. An experimental study of wave run-up at a steep beach. Journal of Fluid Mechanics 486, 161–188.

Kertzscher, U., Seeger, A., Affeld, K., Goubergrits, L., Wellnhofer, E., 2004. X-ray based particle tracking velocimetry–a measurement technique for multi-phase flows and flows without optical access. Flow Measurement and Instrumentation 15 (4), 199–206.

Kikkerta, G., O'Donoghue, T., Pokrajacb, D., Dodd, N., 2011. Experimental study of bore-driven swash hydrodynamics on impermeable rough slopes. Coastal Engineering.

Kimmoun, O., Branger, H., 2007. A particle image velocimetry investigation on laboratory surf-zone breaking waves over a sloping beach. Journal of Fluid Mechanics 588, 353–397.

Lewis, R., 2004. Medical phase contrast x-ray imaging: current status and future prospects. Physics in medicine and biology 49 (16), 3573.

Longuet-Higgins, M. S., 1982. Parametric solutions for breaking waves. Journal of Fluid Mechanics 121, 403–424.

Lucarelli, A., Lugni, C., Falchi, M., Felli, M., Brocchini, M., 2017. On a layer model for spilling breakers: A preliminary experimental analysis. European Journal of Mechanics-B/Fluids.

Melville, W. K., 1996. The role of surface-wave breaking in air-sea interaction. Annual review of fluid mechanics 28 (1), 279–321.

Mo, W., Jensen, A., Liu, P. L.-F., 2013. Plunging solitary wave and its interaction with a slender cylinder on a sloping beach. Ocean Engineering 74, 48–60.

Nydal, O., Pintus, S., Andreussi, P., 1992. Statistical characterization of slug flow in horizontal pipes. International Journal of Multiphase Flow 18 (3), 439–453.

Pedersen, G., Gjevik, B., 1983. Run-up of solitary waves. Journal of fluid mechanics 135, 283–299.

Pedersen, G., Lindstrøm, E., Bertelsen, A., Jensen, A., Laskovski, D., Sælevik, G., 2013. Runup and boundary layers on sloping beaches. Physics of Fluids (1994-present) 25 (1), 012102.

Peregrine, D. H., 1983. Breaking waves on beaches. Annual Review of Fluid Mechanics 15 (1), 149–178.

Pujara, N., Liu, P. L.-F., Yeh, H., 2015. The swash of solitary waves on a plane beach: flow evolution, bed shear stress and run-up. Journal of Fluid Mechanics 779, 556–597.

Rivillas-Ospina, G., Pedrozo-Acuña, A., Silva, R., Torres-Freyermuth, A., Gutierrez, C., 2012. Estimation of the velocity field induced by plunging breakers in the surf and swash zones. Experiments in fluids 52 (1), 53–68.

Rømo, F., Tomasgard, A., Hellemo, L., Fodstad, M., Eidesen, B. H., Pedersen, B., 2009. Optimizing the norwegian natural gas production and transport. Interfaces 39 (1), 46–56.

Russell, J. S., 1845. Report on Waves: Made to the Meetings of the British Association in 1842-43.

Sanchis, A., Johnson, G. W., Jensen, A., 2011. The formation of hydrodynamic slugs by the interaction of waves in gas–liquid two-phase pipe flow. International Journal of Multiphase Flow 37 (4), 358–368.

Scarano, F., 2012. Tomographic piv: principles and practice. Measurement Science and Technology 24 (1), 012001.

Schulkes, R., August 2010. An introduction to multiphase pipe flow.

Sheng, Y., Irons, G., 1991. A combined laser doppler anemometry and electrical probe diagnostic for bubbly two-phase flow. International journal of multiphase flow 17 (5), 585–598.

Smith, L., Jensen, A., Pedersen, G., 2017. Investigation of breaking and non-breaking solitary waves and measurements of swash zone dynamics on a 5° beach. Coastal Engineering 120, 38–46.

Stagonas, D., Warbrick, D., Muller, G., Magagna, D., 2011. Surface tension effects on energy dissipation by small scale, experimental breaking waves. Coastal Engineering 58 (9), 826–836.

Strand, O., 1993. An experimental investigation of stratified two-phase flow in horizontal pipes. Dr. Scient. Thesis, University of Oslo. Oslo, Norway.

Sutherland, P., Melville, W. K., 2013. Field measurements and scaling of ocean surface wave-breaking statistics. Geophysical Research Letters 40 (12), 3074–3079.

Sveen, J., Cowen, E. A., 2004. Quantitative imaging techiques and their application to wavy flows.

Sveen, J. K., 2004. An introduction to matpiv v. 1.6. 1. Preprint series. Mechanics and Applied Mathematics http://urn.nb.no/ URN:NBN:no-23418.

Synolakis, C. E., 1987. The runup of solitary waves. Journal of Fluid Mechanics 185, 523–545.

Taitel, Y., Dukler, A., 1976. A model for predicting flow regime transitions in horizontal and near horizontal gas-liquid flow. AIChE Journal 22 (1), 47–55.

Tanaka, M., 1986. The stability of solitary waves. Physics of Fluids (1958-1988) 29 (3), 650–655.

Tzotzi, C., Andritsos, N., 2013. Interfacial shear stress in wavy stratified gas–liquid flow in horizontal pipes. International Journal of Multiphase Flow 54, 43–54.

Wood, D. J., Pedersen, G. K., Jensen, A., 2003. Modelling of run up of steep non-breaking waves. Ocean engineering 30 (5), 625–644.

Xu, H., Bodenschatz, E., 2008. Motion of inertial particles with size larger than kolmogorov scale in turbulent flows. Physica D: Nonlinear Phenomena 237 (14-17), 2095–2100.

List of Papers

Paper I

L. Smith, G. Pedersen and A. Jensen 'Investigation of breaking and non-breaking solitary waves and measurements of swash zone dynamics on a 5° beach' In: *Coastal Engineering* **120** (2017), pp. 38–46 DOI:10.1016/j.coastaleng.2016.11.004.

Paper II

L. Smith, B. Hu J. Kolaas, K. Sveen and A. Jensen 'X-ray PTV Measurements of Solitary Waves'. In: *Proceedings of the 18th International Symposium on the Application of Laser and Imaging Techniques to Fluid Mechanics. Lisbon Simposia*ISBN 978-989-98777-8-8. Artikkel. s 2604 - 2612

Paper III

L. Smith, J. Kolaas, K. Sveen and A. Jensen 'X-ray measurements of plunging breaking solitary waves' Submitted to *European Journal of Mechanics B/Fluids*, Special Issue: Breaking Waves

Paper IV

L. Smith J. Kolaas, A. Jensen K. Sveen 'Investigation of surface structures in two phase wavy pipe flow by utilizing X-ray tomography' Submitted to *International Journal of Multiphase flow*

Paper V

L. Smith 'A note on PTV measurements in slugs and plugs'

Papers

Paper I

Investigation of breaking and non-breaking solitary waves and measurements of swash zone dynamics on a $5°$ beach.

Lisa Smith, Geir Pedersen, Atle Jensen

II

Paper II

X-ray PTV Measurements of Solitary Waves

Lisa Smith, Bin Hu, Jostein Kolaas, Kristian Sveen, Atle Jensen

III

Paper III

X-ray measurements of plunging breaking solitary waves

Lisa Smith, Jostein Kolaas, Kristian Sveen, Atle Jensen

IV

Paper IV

Investigation of surface structures in two phase wavy pipe flow by utilizing X-ray tomography

Lisa Smith, Jostein Kolaas, Kristian Sveen, Atle Jensen

Paper V

A Note on X-ray PTV of Slugs in Pipes

Lisa Smith